Peptides Modeled on the Transmembrane Region of the Slow Voltage-Gated IsK Potassium Channel: Structural Characterization of Peptide Assemblies in the β-Strand Conformation†

Amalia Aggeli, Neville Boden, Ya-Ling Cheng, John B. C. Findlay, Peter F. Knowles,* Peter Kovatchev, and Paul J. H. Turnbull

Centre for Self-Organising Molecular Systems, The University of Leeds, Leeds, LS2 9JT, U.K.

László Horváth and Derek Marsh

Max-Planck-Institut für biophysikalische Chemie, Abteilung Spektroskopie, D-37077 Göttingen, Germany

Received April 15, 1996⊗

ABSTRACT: A 27-residue peptide, having a sequence corresponding to the transmembrane domain of the IsK protein with slow voltage-gated potassium channel activity, has been incorporated into synthetic saturated-chain phospholipid membranes. The peptide−lipid complexes have been characterized by attenuated-total-reflection Fourier-transform-infrared spectroscopy (ATR-FTIR), spin-label electron spin resonance (ESR) spectroscopy, ^{31}P and ^{2}H nuclear magnetic resonance (NMR) spectroscopy, differential scanning calorimetry, and low-angle X-ray diffraction. From FTIR spectroscopy, it is found that, when reconstituted into membranes by dialysis from 2-chloroethanol, the peptide has a predominantly β-strand secondary structure in which the peptide backbone is oriented at an angle of approximately 56° relative to the membrane normal in dry films of phosphatidylcholines. Hydration of the dry film in the gel phase does not appear to affect the orientation of the peptide backbone, and a relatively small change in orientation occurs when the bilayer undergoes the transition to the fluid phase. The ESR and NMR spectra from spin-labeled and ^{2}H-labeled phospholipids, respectively, indicate that the incorporated peptide restricts the rotational motion of the lipids, without appreciably affecting the chain order, in a way similar to that found for integral membrane proteins. The characteristic two-component ESR spectra from spin-labeled lipids further indicate a selectivity in the interaction of anionic phospholipids with the peptide. The motional restriction of the chains of the spin-labeled phosphatidylcholine and the reduction in the enthalpy of the lipid chain-melting transition indicate that, on average, approximately two to three phospholipid molecules interact directly with each peptide monomer, which is consistent with a limited degree of aggregation of the β-sheet structures. Both ^{31}P NMR spectroscopy and X-ray diffraction indicate that the lipid−peptide complexes have a lamellar structure up to the highest peptide concentration studied ($R_P = 0.2$). The surface area occupied by lipid molecules (ca. 30 Å^2 per chain) in the peptide complexes, deduced from the lamellar repeat spacings at defined water content, is very similar to that in pure fluid lipid bilayers, consistent with the ^{2}H NMR results. The additional membrane surface area contributed by the peptide is approximately 112 Å^2 per monomer. This large value for the peptide area in the fluid bilayer is consistent with the ATR studies of dry peptide/lipid films which suggest that the long axis of the β-strand is strongly tilted with respect to the bilayer normal (56° in the dry film).

β-Secondary structure is an important feature in globular proteins. It is found as antiparallel sheets or barrels in one class of protein, termed "β proteins," or as parallel sheets or barrels in proteins having a mixed composition of α-helices and β-strands, termed "α/β proteins" (Branden & Tooze, 1991). This classification may hold also for membrane proteins where porins with a 16-stranded antiparallel β-structure would exemplify the "β" class (Weiss et al., 1991) and acetylcholine receptor (Unwin, 1993) the "α/β" class. There is major interest in whether β-secondary structure has a role in the function of the *Shaker* class of potassium ion channel proteins (Yellen et al., 1991; Bogusz et al., 1992) and in the glucose transporter (Fischbarg et al., 1993).

The medical importance of β-secondary structure as a diagnostic indicator or possible cause of certain neurological disorders has also been recognized. Thus, in the scrapie class of disorders (which includes bovine spongiform encephalopathy, BSE, and Creutzfeld−Jakob disease), the transformation from normal to the diseased state appears to involve a mutation in a membrane protein which leads to a dramatic increase in the content of β-domains and in the deposition of oligopeptide "β-plaques" (Prusiner, 1991; Pan et al., 1993). Similar deposits of oligopeptide having predominantly β-structure and termed "β-amyloid plaques" are diagnostic of Alzheimer's disease (Barrow & Zagorski, 1991).

There is a general paucity of information on the structure of proteins and peptides in membranes. This is due in part to the difficulties in obtaining suitable two- and three-

† This work has been supported by grants from the SERC (to N. Boden, J. B. C. Findlay, and P. F. Knowles) and the British−German Academic Research Collaboration (ARC) programme (to P. F. Knowles and D. Marsh).

⊗ Abstract published in *Advance ACS Abstracts,* November 15, 1996.

S0006-2960(96)00891-4 CCC: $12.00

FIGURE 1: Primary structures of *K27* and *K26*.

dimensional crystals for study by electron cryomicroscopy or X-ray crystallography, respectively. High-resolution nuclear magnetic resonance (NMR),[1] which is a major technique for determination of atomic resolution structures in solution, is unsuited to the study of peptide and protein structures in membranes while solid-state NMR, which is capable of addressing such structural questions, has been applied successfully in only a limited number of cases (Cross & Opella, 1994).

In view of these difficulties in structure determination, alternative strategies are required. The determination of the structure of peptide assemblies in membranes by spectroscopic and other physical methods would represent an important advance.

The present paper describes how such structural information can be deduced from use of a range of spectroscopic and allied techniques. The peptide chosen for study, termed *K27*, is modeled on the transmembrane segment of the slow voltage-gated (IsK) class of K^+ channel proteins (Takumi et al., 1988); a mutant form of this peptide, termed *K26* (whose primary structure differs from that of *K27* only by the omission of a leucine residue found at position 2 of *K27*), was also studied. Both peptides are highly nonpolar (see Figure 1) and adopt almost completely β-secondary structure when reconstituted into DMPC and DPPC membranes by dialysis from organic solvents.

MATERIALS AND METHODS

Materials. Dipalmitoylphosphatidylcholine (DPPC) and dimyristoylphosphatidylcholine (DMPC) were obtained from Lipid Products (Surrey, England) as chloroform/methanol solutions. DMPC for the ESR studies was obtained from Fluka (Buchs, Switzerland). DMPC perdeuterated in the *sn*-2 chain (DMPC-d_{27}) was synthesized according to Gupta et al. (1977) and Mason et al. (1981).

Lipid purity, as analyzed by thin-layer chromatography before and after experiments, showed that lysophosphatidylcholine and fatty acid degradation products were absent.

Peptide Synthesis and Purification. Synthesis of peptides employed the continuous-flow, fluorenylmethoxycarbonyl (FMOC) polyamide, solid-phase method using the standard manufacturer's protocols on a MilliGen/Biosearch 9050 peptide synthesizer. PepSyn-KA resins, prederivatized with the FMOC-protected C-terminal amino acid of the desired peptide, and preformed FMOC-amino acid-pentafluorophenol (Pfp) esters [or preformed dihydroxybenzotriazole esters of FMOC-Ser(tBut) and FMOC-Thr(tBut), where the side-chain hydroxyls are protected as the tertiary butyl derivatives] were used at 4-fold excess to give 0.1 mmol scale syntheses. Couplings were controlled by the counterion distribution monitoring system (CDM) to achieve not less than 99% coupling efficiency. Default deprotection protocols were extended to 15 min. After completion of the synthesis, the resin was extensively washed with about 150 mL of each of *tert*-amyl alcohol, glacial acetic acid, *tert*-amyl alcohol followed by washing with about 300 mL of diethyl ether. The washed resin was vacuum-dried overnight. Resin cleavage and side-chain deprotection were achieved with Reagent K (0.1 mL/mg of resin) for 2.5 h as reported by King et al. (1990) except that 87.5% anhydrous trifluoroacetic acid (TFA) was used instead of 82.5% TFA. The cleaved resin was filtered and washed further with 87.5% TFA. The filtrate was rotary-evaporated at room temperature until all TFA was removed. The gel-like residue was dissolved in hexafluoroisopropyl alcohol, HFIP (2 mL), extruded into diethyl ether (50 mL), and centrifuged (Microfuge, 4000 rpm, 5 min, 4 °C). The pellet was washed 6 times, by resuspension in fresh diethyl ether and centrifugation, before being dried overnight under vacuum. The peptide was dissolved in HFIP (about 1 mL), diluted to 100 mL with deionized water, and freeze-dried for storage. High-resolution ^{1}H NMR on the peptide dissolved in ^{2}H methanol indicated that it was free of low molecular weight organic impurities. Peptide quantitation was carried out using the bichinchoninic acid, BCA (Smith et al., 1985), or manual ninhydrin (Hirs, 1967) assays.

Attempts have been made to purify the peptides by reverse-phase HPLC, but difficulties have been encountered due to their highly nonpolar character. Initially, a C_{18} resin was used, but no peptide could be recovered. When a less hydrophobic column (C_4) was used, the peptide was adsorbed using 0.1% TFA in methanol as solvent, but low yields of peptide (10%) were achieved during elution, even with the best solvent identified (0.1% TFA in propan-2-ol). Because of these poor yields, HPLC was not used further in the purification. The HPLC elution profile, however, indicated a single peptide species, and the sequencing data (see later) on the peptide purified by the rigorous extraction and precipitation procedures described were judged acceptable. Elemental analysis (51.4 $\pm$ 0.3% C, 6.0 $\pm$ 0.3% H, 10.6 $\pm$ 0.4% N, 6.9 $\pm$ 2.0% F) was in close agreement with predictions from the empirical formula assuming the presence of TFA at a TFA/*K27* mole ratio of 4.4 $\pm$ 1.3 and water at a water/*K27* mole ratio of 9.7 $\pm$ 3.5 (51.4% C, 6.2% H, 11.2% N, 6.9% F). However, when dialyzed in the presence of lipid against water from a solution of 2-chloroethanol, the peptide was found to be free of fluorine (from the cleavage reagent) as analyzed by ^{19}F NMR.

Peptide Sequence Analysis. Peptides were sequenced using both solid-phase and liquid-pulse sequencing strategies. For solid-phase sequencing, the peptide (dissolved in 1% HFIP/water) was dried onto a Sequelon arylamine membrane disk at 56 °C. Covalent coupling was achieved with 1-ethyl-3-[3-(dimethylamino)propyl]carbodiimide (10 μL, 10 mg/

[1] Abbreviations: 14-PCSL, 14-PSSL, and 14-PASL, spin-labeled phosphatidylcholine, phosphatidylserine, and phosphatidic acid bearing the nitroxide group on the 14th carbon atom of the *sn*-2 chain; ATR-FTIR, attenuated-total-reflection Fourier-transform-infrared spectroscopy; DMPC, dimyristoylphosphatidylcholine; DPPC, dipalmitoylphosphatidylcholine; DMPC-d_{27}, dimyristoylphosphatidylcholine perdeuterated in the *sn*-2 chain; DSC, differential scanning calorimetry; ESR, electron spin resonance; FTIR, Fourier-transform-infrared spectroscopy; *K27*, a 27-residue peptide with a sequence based on the transmembrane segment of the IsK protein; *K26*, a 26-residue peptide whose primary structure differs from that of *K27* only by the omission of the leucine residue at position 2 of *K27*; NMR, nuclear magnetic resonance; *R*, dichroic ratio of a given band in ATR-FTIR spectrum.

mL) in MES buffer (pH 5.0), dried onto the disk at room temperature (about 30 min). The membrane-coupled peptide was subjected to automated solid-phase Edman degradation on a MilliGen/Biosearch 6600 ProSequencer. The phenylthiohydantoin-amino acids were identified (at 269 nm) by reverse-phase HPLC (Waters SequeTag C_8 column) on a Waters 600 system, using a gradient of acetonitrile in 30 mM ammonium acetate, pH 4.8.

Liquid-pulse sequencing was carried out on an Applied Biosystems 477A protein sequencer linked to an Applied Biosystems 120A analyzer. TFA-pretreated, glass-fiber disks were preconditioned using Biobrene (30 μL) which was dried onto the surface of the disk before the disk was subjected to 3 sequencing cycles. Peptide samples (generally 25 μL aliquots of 0.1−1 nmol in 1% HFIP/water) were dried onto the preconditioned disks under nitrogen. Sequencing was carried out using the approved Applied Biosystems methodology. Each batch of peptide was subjected to a few cycles of liquid-pulse sequencing to assess the probable purity, using a figure of 90% correct N-terminal residue as the minimum criterion for acceptability of the peptide.

Preparation of Peptide/Lipid Complexes. The required amounts of peptide and lipid were codissolved in freshly distilled 2-chloroethanol and dialyzed against 3 × 2 L changes of either distilled water or 0.1 M NaCl, 2 mM Hepes, and 1 mM EDTA, pH 7.4, in the case of the samples for ESR spectroscopy, over a period of 24 h [cf. Brophy et al. (1984)]. The peptide/lipid complexes were collected as pellets by centrifugation and resolved from any free lipid by suspending the pellet in 1.0 M NaCl, 2 mM Hepes, and 1 mM EDTA, pH 7.4, centrifuging, and discarding the supernatant. The final pellets for all studies except ESR spectroscopy were suspended in distilled water and dialyzed for a further 24 h period against 3 × 2 L changes of distilled water. The peptide/lipid complexes prepared by this procedure were found to sediment as a single band on continuous sucrose gradient centrifugation (10−55% sucrose). For preparation of samples at limited hydration, the dialyzed material was freeze-dried overnight to give a white powder, to which the requisite amount of D_2O (FTIR samples) or H_2O was then added via a microsyringe, the hydrations of the samples being determined gravimetrically. Thereafter, the glass sample tubes were flame-sealed, and the rehydrated samples were held at 40 °C for 2 days and mixed by centrifugation until homogeneous in appearance. For all studies other than ESR, peptide/lipid ratios in reconstituted samples were determined by assay of phosphate (Bartlett, 1959) and protein (Hirs, 1967).

FTIR Spectroscopy. FT-IR spectra were recorded on a Perkin-Elmer 1760X spectrometer at a resolution of 4 cm^{-1}. A homemade thermostated cell with a CaF_2 window was used for all experiments. Limited hydration samples (hydrated with D_2O) were placed directly on the center of two CaF_2 windows, and 32 scans were accumulated for each spectrum.

ATR-FTIR studies were performed using a Specac variable-angle ATR attachment and a ZnSe crystal (64.2 × 12 × 4.2 mm) with angle of incidence 45° giving 14 internal reflections. Temperature control was achieved by circulating water via a thermostated bath (Colora, WK3) through a homemade cell which housed the ATR crystal. The vesicle suspension was added to a thin film of lipid which had been deposited on a ZnSe ATR crystal by evaporation from a chloroform solution. Water was removed by slow evaporation. For hydrated samples of *K27*/DMPC, the film was rehydrated with D_2O and incubated at 40 °C for 2 h prior to acquisition of spectra. This procedure eliminates interference from H_2O in the peptide amide I region of the ATR spectra. The water content of these hydrated oriented samples was estimated to be consistent with excess hydration (D_2O/lipid mole ratio >35). This estimate was based upon the intensities of the O−D stretching band at 2490 cm^{-1} and the lipid carbonyl stretching band at 1734 cm^{-1} in the ATR spectra of the hydrated samples for both 0° and 90° polarized incident radiation. On the basis of these intensities, the corresponding intensity ratios of the two bands in equivalent unoriented samples were determined (Ohta & Iwamoto, 1985), and these were compared to the band ratio observed in an unoriented sample of known hydration. The ATR spectra were recorded for 0° or 90° polarization with respect to the plane of incidence with a Specac KRS-5 polarizer, and 200 scans were accumulated for each spectrum. Spectra of the bilayer films were corrected for absorption by the ZnSe crystal, and a second-derivative procedure was applied to enhance their resolution.

A curve-fitting procedure was used to fit the bands of the spectrum in the region 1500−1700 cm^{-1} to individual lines with both Lorentzian and Gaussian components of varying magnitude in order to determine secondary structure content and the corresponding dichroic ratios.

Given the method used for deposition of samples onto the ATR crystal, in calculating the electric field amplitudes a thick film approximation was used which considered only the ATR crystal and peptide/lipid media. The values of the refractive indices used for these calculations were taken to be 2.4, 1.4, and 1.5 for the ZnSe crystal, the peptide, and the lipid, respectively (Fringeli, 1977; Frey & Tamm, 1991).

ESR Spectroscopy. Spin-labeled phosphatidylcholine (14-PCSL), phosphatidylserine (14-PSSL), and phosphatidic acid (14-PASL), bearing the nitroxide group on the 14th carbon atom of the *sn*-2 chain, were synthesized according to Marsh and Watts (1982). The peptide/lipid complexes formed by dialysis were homogeneous on continuous sucrose density gradient centrifugation after sedimenting through 1 M NaCl. Lipid phosphorus and protein were assayed according to Eibl and Lands (1969) and Lowry et al. (1951), respectively. The complexes were resuspended in 2 mM Hepes, 1 mM EDTA, pH 8.3, and "doped" with spin-labeled lipid by adding 5 μg of spin-label in ethanol per 2 mg of lipid in the sample. Unincorporated spin-label was removed by centrifugation and washing with the sample buffer. The samples were transferred to 1 mm i.d. glass capillaries which were flame-sealed prior to study.

Spectra were recorded on a Varian Century Line 9 GHz ESR spectrometer with nitrogen gas flow temperature regulation [see Marsh (1982)]. Quantitation of the relative populations of the two spectral components was performed by integration and by digital subtraction (Marsh, 1982) using the spectrum for pure lipid as reference.

Differential Scanning Calorimetry (DSC). Samples were hermetically sealed in Perkin-Elmer large-volume capsules, and DSC thermograms were obtained using a Perkin-Elmer DSC-2 calorimeter equipped with an Intracooler 1 subambient temperature controller and operating at a heating rate of 5 K·min^{-1}. Temperature and enthalpy calibrations were made using an indium standard. For enthalpy determinations,

the areas under the excess heat capacity curves were determined by planimetry, and any changes in heat capacity observed during the course of the transition were taken to occur at the transition temperature (Guttman & Flynn, 1973).

^{31}P and ^{2}H NMR Spectroscopy. Both ^{31}P and ^{2}H NMR spectra were recorded at 40 °C on a Bruker MSL-300 spectrometer operating in the quadrature detection mode. Samples at excess hydration were contained in 10 mm o.d. NMR tubes. The limited hydration samples were flame-sealed in a 7 mm o.d. sample tube with a rubber plug covered in PTFE tape placed inside, directly above the sample to prevent loss of water. The 7 mm tube was then placed inside a 10 mm o.d. NMR tube containing distilled water to minimize temperature gradients. ^{31}P NMR spectra were acquired using a single-pulse sequence with a pulse length of 5 μs equivalent to a pulse angle of approximately 45°, a recycle delay of 2 s, and a spectral width of 50 kHz; the proton broad-band decoupling power (approximately 8 W) was switched on only during the FID acquisition period (approximately 40 ms). ^{2}H NMR spectra were acquired using the solid-echo pulse sequence [90°$-\tau-$90°$-\tau-$FID]; an average 90° pulse of 9 μs was used with a pulse separation of 18 μs, a recycle delay of 350 ms, and a spectral width of 250 kHz.

Low-Angle X-ray Diffraction. Samples were flame-sealed in 0.7 mm o.d. glass capillaries, and low-angle X-ray diffraction patterns were obtained at 40 °C using nickel-filtered CuKα X-radiation collimated by a "home built" pin-hole camera. Temperature control was achieved by the circulation of a water/ethylene glycol mixture through the sample holder via a thermostated bath (Colora WK3). The sample temperature was determined by the use of a copper/constantan thermocouple in series with an identical reference thermocouple in a distilled water/ice bath. Distance between sample and photographic plate was determined using a potassium aluminum sulfate calibrant (Sandbank, 1986). A typical exposure time of 3 h was required to observe the low-angle diffraction pattern from the one-dimensional lattice of lipid bilayers. Intensities of the X-ray diffraction patterns were measured on a Hilger and Watts microphotometer connected to a chart recorder.

RESULTS AND INTERPRETATION

FTIR Spectroscopy. The conformation of both *K27* and *K26* reconstituted into DMPC bilayers at high peptide/lipid ratios (R_P) of approximately 0.1 is mainly β-strand as judged by the presence of one amide I band at approximately 1627 cm^{-1} in the nonoriented FTIR spectrum (data not shown), with only a small band at approximately 1656 cm^{-1} indicating minimal amounts of α-helix (Miyazawa & Blout, 1961; Surewicz & Mantsch, 1988; Byler & Susi, 1986). Contributions to this minor component might also come from loop structures (Surewicz et al., 1993). Estimates from band fitting indicate that the β-strand conformational content is at least 85%, depending on the peptide/lipid ratio.

The ATR-FTIR spectra of oriented *K27*/DMPC bilayers recorded with incident radiation polarized at 0° (upper spectrum) and 90° (lower spectrum) relative to the plane of incidence are shown in Figure 2a and Figure 2b for the dry film at 20 °C and the fluid phase at 40 °C, respectively.

The orientation of the lipid chains in dry films and, in the case of DMPC, in the gel phase has been established from

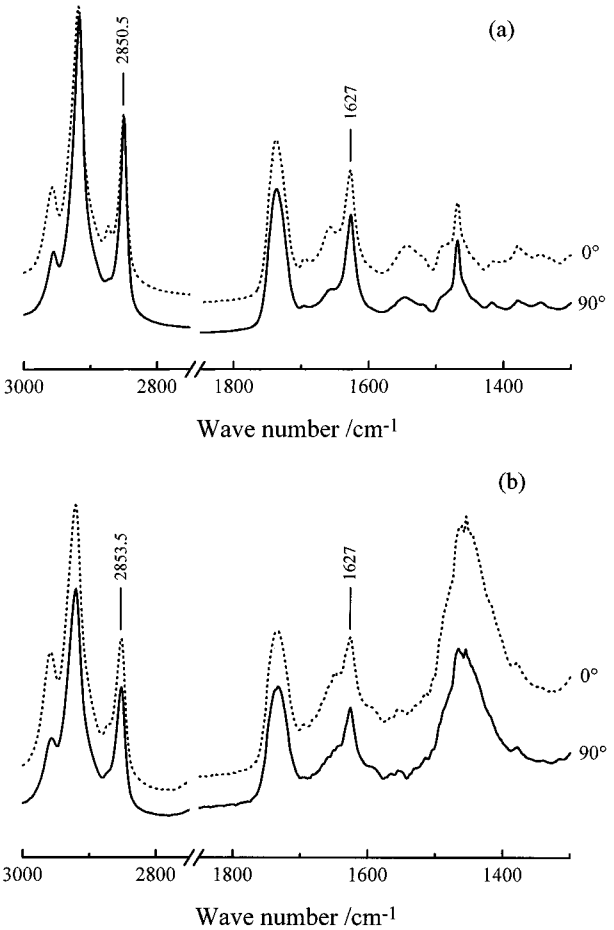

FIGURE 2: ATR-FTIR spectra of oriented *K27*/DMPC bilayers at (a) 20 °C (dry film) with $R_P \approx 0.04$ and (b) 40 °C (fluid; hydrated) with $R_P \approx 0.03$. The upper and lower spectra are for incident radiation polarized at 0° and 90°, respectively, with respect to the plane of incidence. The amide I band for the β-strand in the 1627 cm^{-1} region is indicated for both gel and fluid bilayers as is the lipid symmetric CH_2 stretching band in the 2850−2854 cm^{-1} region.

the polarization of the symmetric CH_2 stretching band. This absorption is seen in both the 0° and 90° polarization in Figure 2a,b between 2850 and 2854 cm^{-1}. As can be seen from Table 1, the value of the dichroic ratio (R) for this band in the dry films of both DMPC and DPPC was found to be between 0.86 and 0.90 in both the presence and absence of *K27*, suggesting that the incorporation of the peptide has a negligible effect upon the orientation of the lipid chains. Likewise, the addition of D_2O at room temperature has no significant effect on chain orientation as judged by comparison of the values of R for DMPC in the dry film and gel phase. Taking the angle between the absorption dipole moment of the CH_2 stretching band and the long axis of the hydrocarbon chains to be 90° (Fringeli & Günthard, 1981), the observed values of R are consistent with a lipid chain tilt angle, ϑ, of approximately 32° with respect to the bilayer normal. This is in good agreement with the values previously determined by X-ray diffraction (Janiak et al., 1976, 1979) for both DMPC and DPPC in the gel phase. The lipid chain order parameter, $^1/_2(3\langle\cos^2\vartheta\rangle - 1)$, derived from the ATR measurements is 0.45 for *K27*/DMPC in the fluid phase, compared with a value of 0.60 for the chains in the gel phase.

The values of R for the amide I and amide II bands at 1626 and 1538 cm^{-1}, respectively, have been determined by curve-fitting and are also summarized in Table 1. Due to the nature of the β-sheet conformation, it is not generally

Table 1: Summary of Dichroic Ratios for Peptide and Lipid Chains in Various Phases, As Determined from ATR-FTIR

	DMPC dry film 20 °C	DPPC dry film 20 °C	*K27*/DPPC ($R_P = 0.05$) dry film 20 °C	*K27*/DMPC ($R_P = 0.04$) dry film 20 °C	*K27*/DMPC ($R_P = 0.04$) gel phase 20 °C	*K27*/DMPC ($R_P = 0.04$) fluid phase 40 °C
CH_2 stretching	0.87 ± 0.04	0.90 ± 0.04	0.87 ± 0.04	0.89 ± 0.04	0.86 ± 0.04	1.09 ± 0.04
amide I	−	−	1.05 ± 0.04	1.05 ± 0.04	1.07 ± 0.04	1.17 ± 0.04
amide II	−	−	1.7 ± 0.3	1.9 ± 0.3	N/O	N/O

possible to determine the peptide strand tilt angle with respect to the bilayer solely from the value of R for the amide I band. The symmetry and phase relations of the coupled infrared-active vibrations in a β-sheet require that the resultant transition moment for the amide modes be oriented either parallel or perpendicular to the β-strand axis (Miyazawa, 1960; Fraser & MacRae, 1973). The transition moment for the amide I band is oriented perpendicular to the molecular axis (Gremlich et al., 1983), and hence the value of R will depend on both the strand and transition moment orientations with respect to the sheet and, in general, also on the sheet orientation with respect to the bilayer normal. Therefore, in dry films of *K27*/DMPC and *K27*/DPPC, the strand orientation, γ, with respect to the bilayer normal has been estimated from the value of R for the amide II band because the transition moment for this band lies along the peptide strand axis (Miyazawa, 1967; Krimm & Bandekar, 1986). The dichroic ratio for a transition moment oriented along the strand axis is given by

$$R_{\text{amideII}} = \frac{E_x^2}{E_y^2} + \frac{E_z^2}{E_y^2}\frac{2\langle\cos^2\gamma\rangle}{1-\langle\cos^2\gamma\rangle} \qquad (1)$$

for a 45°-cut ATR plate where E_x, E_y, and E_z are the components of the electric field vector of the incident radiation. Equation 1 is obtained by using the method given in Ahn and Frances (1992) with the transformation matrices from Zbinden (1964) and integration over the azimuthal orientation, ϕ, of the strand axis in the bilayer axis system. The angular brackets in eq 1 indicate that the value of $\cos^2\gamma$ is integrated over a possible distribution of orientations of the strand axes. Taking the value of $R \approx 1.9$ for the amide II band in dry films of both *K27*/DMPC and *K27*/DPPC translates to an effective strand tilt angle of approximately $\gamma = 56°$ ($\langle\cos^2\gamma\rangle = 0.32$) with respect to the bilayer normal in the dry films, assuming a unique strand orientation or a narrow distribution of orientations. The fact that the dichroic ratios of the amide I and amide II bands have different values (Table 1) indicates that the β-strands are not randomly oriented. Also, the value deduced for the β-strand orientation ($\gamma = 56°$) does not imply that the planes of the β-sheets are randomly tilted with respect to the bilayer normal.

In the gel- and fluid-phase bilayer, determination of R for the amide II band and hence the peptide strand orientation was prevented by the presence of D_2O which caused the amide II band to shift to the 1400−1500 cm^{-1} region due to N−H ↔ N−D exchange and therefore be obscured by the lipid CH_2 bending band centered at 1460 cm^{-1}. Hydration with H_2O instead of D_2O did allow the amide II band to be observed in the gel and fluid phases. Unfortunately, the presence of the large O−H bending band centered at 1645 cm^{-1} not only obscured the amide I band but also distorted the base line in the amide II region to such a degree as to prevent determination of the dichroic ratio of the latter. However, from a comparison of the values of R for the amide I band (Table 1), it would appear that addition of water to the dry peptide/lipid film below the lipid chain melting transition causes no significant change in the peptide strand orientation, and elevating the temperature of the hydrated bilayer above the lipid chain melting transition produces only a relatively small change.

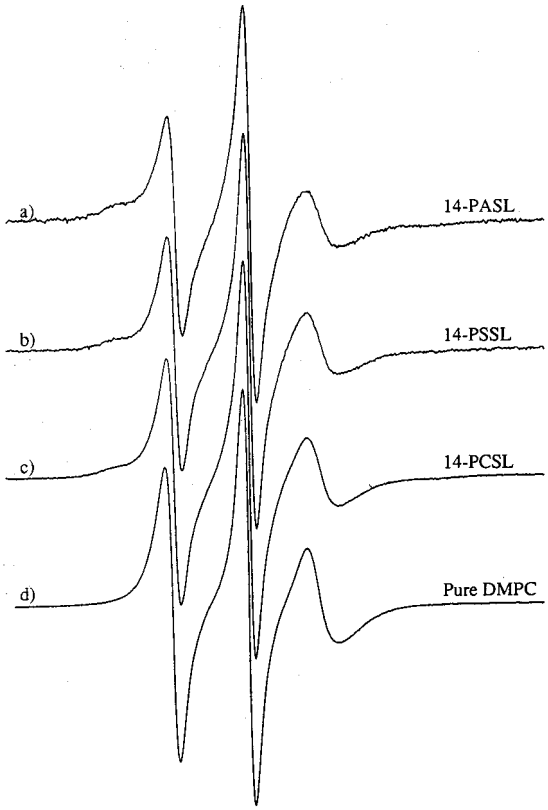

FIGURE 3: ESR spectra of (a) the 14-PASL phosphatidic acid spin-label, (b) the 14-PSSL phosphatidylserine spin-label, and (c) the 14-PCSL phosphatidylcholine spin-label, at 30 °C and a relative concentration of ca. 1 mol % in complexes of *K27*/DMPC at R_P = 0.12, and of (d) 14-PCSL in DMPC alone at 25 °C. Total scan range = 100 G.

ESR Spectroscopy. Figure 3a−c shows the ESR spectra of the phosphatidylcholine (14-PCSL), phosphatidylserine (14-PSSL), and phosphatidic acid (14-PASL) spin-labels in complexes of the *K27* peptide with DMPC at $R_P = 0.12$. The spectra were recorded at 30 °C which is above the chain melting phase transition of DMPC. The spectra are all composed of two components, one of which is characteristic of the spin-label in fluid bilayers (cf. Figure 3d). The other component, which is resolved in the outer wings of the spectrum, has a large spectral anisotropy that indicates a strong restriction in the rotational motion of the spin-labeled lipid chains on the conventional nitroxide ESR time scale [see, e.g., Marsh (1981)]. These ESR spectral effects are

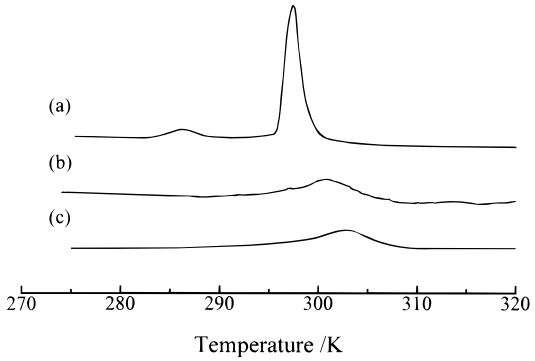

FIGURE 4: DSC thermograms, at 5 K·min^{-1} heating rate, for (a) DMPC at excess hydration, (b) *K27*/DMPC with $R_P = 0.2$ at excess hydration ($R_W > 35$), and (c) *K27*/DMPC with $R_P = 0.2$ at limited hydration ($R_W = 35$).

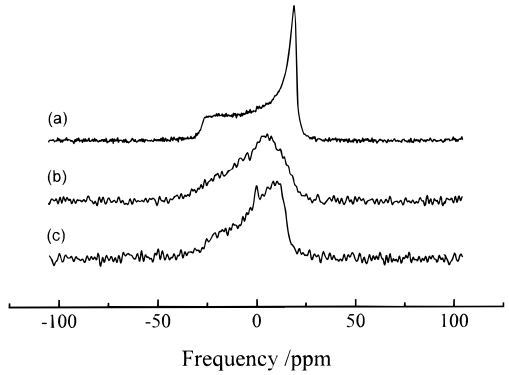

FIGURE 5: ^{1}H-Decoupled ^{31}P NMR spectra at 40 °C for (a) DMPC-d_{27} at excess hydration, (b) *K27*/DMPC-d_{27} with $R_P = 0.2$ at excess hydration ($R_W > 35$), and (c) *K27*/DMPG-d_{27} with $R_P = 0.2$ at limited hydration ($R_W = 35$).

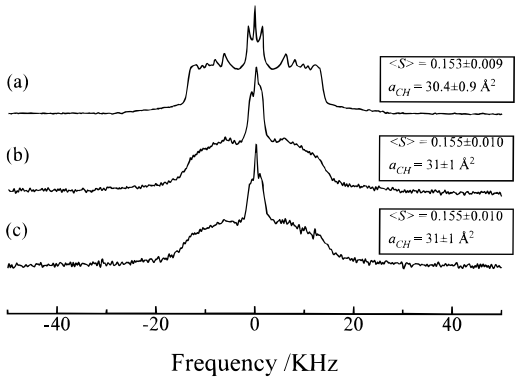

FIGURE 6: ^{2}H NMR spectra at 40 °C for (a) DMPC-d_{27} at excess hydration, (b) *K27*/DMPC-d_{27} with $R_P = 0.2$ at excess hydration ($R_W > 35$), and (c) *K27*/DMPC-d_{27} with $R_P = 0.2$ at limited hydration ($R_W = 35$).

very similar to those found for a wide variety of integral membrane proteins, for which the motionally restricted component has been attributed to those lipid chains that are directly in contact with the intramembranous hydrophobic surface of the protein [cf. Marsh (1985)]. The present results therefore suggest strongly that the assemblies of the *K27* peptide are integrated in the lipid bilayers in such a way as to present a hydrophobic surface to the lipid chains that is very similar to that of integral proteins in biological membranes.

Although ESR spectra of the different spin-labeled lipids all possess the same qualitative two-component features, they differ considerably in the relative proportions of the motionally restricted spin-label population. By spectral subtraction, the fractional populations are found to be in the ratio 1.7:1.3:1 for phosphatidic acid, phosphatidylserine, and phosphatidylcholine, respectively. Because the peptide complexes all have the same peptide/lipid ratio, this is clear evidence for a selectivity between the different spin-labeled lipid species for occupation of sites at the peptide/lipid interface. The selectivity demonstrated for negatively charged lipids implies that the peptide is incorporated into the bilayer in such a way that the positively charged residues at the N- and C-termini are located in a region close to the phospholipid headgroups. Assuming that the spin-labeled phosphatidylcholine displays no selectivity relative to the parent unlabeled DMPC host lipid, as has been found for a wide range of lipid/protein systems, the fraction of motionally restricted component in the spectrum of Figure 3c (obtained from spectral subtraction) corresponds to approximately 2.5 ± 0.7 lipid sites per peptide monomer at which the lipid chain mobility is restricted by direct interaction with the intramembranous surface of the peptide assemblies.

Differential Scanning Calorimetry. The DSC thermograms for pure DMPC and *K27*/DMPC at $R_P = 0.2$ are shown in Figure 4. The incorporation of the peptide into DMPC bilayers abolishes the low enthalpy pretransition and causes a significant broadening of the chain melting transition and a reduction in its enthalpy. Such effects are similar to those observed with other peptides and membrane proteins (Chapman et al., 1977; Chapman, 1983). They are consistent with the peptide reducing the cooperativity of the transition, by causing defects in the packing of the lipid chains (Seelig & Seelig, 1980), and immobilizing those lipid molecules with which it is in direct contact such that they no longer take part in the transition (Chapman, 1983). On the basis of the observed reduction in enthalpy, it is estimated that the number of lipid molecules per peptide monomer that are removed from the transition is approximately 3.0 with a confidence limit of ±0.8. This value compares favorably with the value of 2.5 determined by ESR.

^{31}P NMR Spectroscopy. Figure 5 shows the effect of *K27*, at $R_P = 0.2$, upon the ^{1}H-decoupled ^{31}P NMR spectra of fluid DMPC bilayers. The spectra in the presence and absence of peptide all have an axial chemical shielding anisotropy (CSA) of negative sign, which is consistent with a bilayer arrangement of the lipid [cf. Seelig (1978)]. The magnitude of the CSA is reduced slightly by the presence of the peptide from a value of approximately −45 ppm to approximately −38 ppm (Figure 5c). The peptide does, however, have a marked effect on the spectral line shape due to broadening of the intrinsic line widths. This is consistent with a decrease in the rate of reorientational motion of the lipid headgroups, together with either a limited increase in their disorder or a limited change in their time-averaged orientation or conformation.

^{2}H NMR Spectroscopy. The ^{2}H NMR spectra for DMPC-d_{27} and *K27*/DMPC-d_{27} at $R_P = 0.2$ are given in Figure 6. The spectra for samples containing peptide show a considerable increase in line broadening and a decrease in resolution, without any appreciable change in the overall spectral splitting, at both excess and limited hydrations. This suggests either, as with the ^{31}P NMR, a considerable slowing down of the reorientational motion or a greater distribution of order parameters [cf. Seelig and Seelig (1980)]. However, unlike

the ^{31}P NMR spectra, it would appear, from the similarity in the overall anisotropy of the ^{2}H NMR spectra for pure DMPC and *K27*/DMPC, that the peptide does not significantly perturb the packing of the lipid chains at either limited hydration, in this case a water/lipid mole ratio (R_W) of 35, or excess hydration. These observations are consistent with those made on the interaction of lipids with integral proteins (Oldfield, 1988; Davis, 1983) but contrast with the effects on lipid order of peptides, such as gramicidin (Rice & Oldfield, 1979; Watnick & Chan, 1990).

For perdeuterated chains, it is possible to estimate the average C−D bond order parameter, $\langle S \rangle$, from the first moment of the quadrupolar splittings, $\langle \Delta \upsilon \rangle$

$$\langle S \rangle = \frac{4}{3} \chi^{-1} A^{-1} \langle \Delta \upsilon \rangle \tag{2}$$

where χ is the quadrupolar coupling constant (170 kHz) and A is equal to $2/3\sqrt{3}$ (Bienvenue et al., 1982). This yields values of $\langle S \rangle = 0.155 \pm 0.010$ for *K27*/DMPC-d_{27} with $R_P = 0.2$ at both excess hydration and limited hydration of $R_W = 35$, compared with a value of $\langle S \rangle = 0.153 \pm 0.009$ for pure DMPC bilayers. Thus, there is little or no change in the average lipid chain order on interaction with the peptide, although a change in the distribution of order parameters of the chain segments cannot be excluded.

It has been shown by Boden et al. (1991) that the average C−D bond order parameter (excluding the first methylene and terminal methyl groups) for chain-deuterated lipids in fluid bilayers is approximately proportional to the inverse of the average lipid chain surface area, a_{CH}. A calibration made with pure fluid DMPC bilayers at 40 °C and various hydrations below the swelling limit yields a linear relationship between $1/a_{CH}$ (determined from X-ray diffraction) and $\langle S \rangle$:

$$\frac{1}{a_{CH}} = m\langle S \rangle + c \tag{3}$$

where $m = 0.0667 \pm 0.0055$ Å^{-2} and $c = 0.0227 \pm 0.0010$ Å^{-2}.

Applying this calibration to the data for the peptide/lipid complexes yields a value of $a_{CH} = 31 \pm 1$ Å^2, which is essentially the value for pure fluid DMPC bilayers, as expected from the similarity in the values of $\langle S \rangle$.

Low-Angle X-ray Diffraction. The X-ray diffraction patterns for the peptide/lipid complexes, at limited hydration, show lamellar order (data not shown). From the measured lamellar repeat distances, D, and the composition of the lamellar phase, it is possible to determine the average bilayer surface area per lipid molecule, $\langle A \rangle$ [cf. Luzzati (1968)], which is defined in eq 4:

$$\langle A \rangle = 2 \frac{\sum_i R_i V_i M_i}{N_A D} \tag{4}$$

where N_A is the Avogadro number and M_i, V_i, and R_i are respectively the molar masses, partial specific volumes, and mole ratios, with respect to lipid, of component i, which in this case may be lipid, peptide, or water (for lipid, $R_i = 1$). The partial specific volume of DMPC at 40 °C was taken to be 0.987 mL/g (Nagle & Wilkinson, 1978), and, based on amino acid composition, a partial specific volume of 0.75 mL/g was estimated for the peptide. For pure lipid bilayers, $\langle A \rangle$ is simply equal to a_L, the cross sectional area of the lipid projected onto the bilayer surface (equal to $2a_{CH}$), but in the presence of another molecule such as a peptide or protein, it is defined as in eq 5:

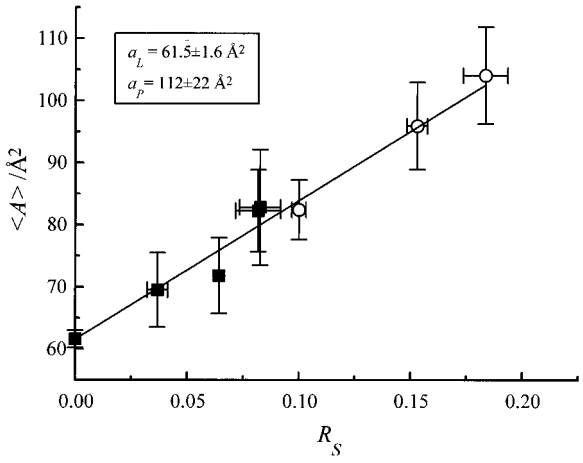

FIGURE 7: Plot of average bilayer surface area per lipid, $\langle A \rangle$, against peptide/lipid ratio, R_P, at 40 °C for (■) *K26*/DMPC bilayers with $R_W = 25$ and (○) *K27*/DMPC bilayers with $R_W = 35$.

$$\langle A \rangle = a_L + 2a_P R_P \tag{5}$$

where a_P is the average area per peptide monomer projected onto the bilayer surface, assuming each monomer spans the bilayer.

The dependence on peptide/lipid ratio of the mean area per lipid molecule, determined from the measured spacings (cf. eq 4), is given in Figure 7 for *K27*/DMPC and *K26*/DMPC bilayers at 40 °C. As can be seen, both data sets lie approximately on the same straight line, indicating that the value of a_P for both *K26* and *K27* when in the β-strand conformation in the membrane is approximately the same. On the basis of eq 5, it can be seen that the linear variation of $\langle A \rangle$ with R_P indicates that the area per lipid is independent of R_P, which is in agreement with the ^{2}H NMR results for the area per chain. Therefore, a_P is equal to half the gradient of the linear fit to the data in Figure 7 and is calculated to be 112 ± 22 Å^2.

DISCUSSION

The *K27* peptide incorporated into DMPC by dialysis from 2-chloroethanol forms peptide/lipid complexes with a lamellar membrane structure, as evidenced both by ^{31}P NMR and by X-ray diffraction. The incorporated *K27* peptide assemblies affect the mobility of the lipids in much the same way as do native integral membrane proteins (Marsh, 1985; Bloom & Smith, 1985). A motionally restricted component attributable to lipids in direct contact with the intramembranous peptide assemblies is resolved from the fluid bilayer lipid component in the spin-label ESR spectra [cf. Marsh (1985) and Peelen et al. (1992)]. The ^{2}H NMR spectra show that there is no change in the average lipid chain order in the *K27* peptide/lipid complexes, but a considerable slowing down of the chain motion, relative to that in pure lipid bilayers [cf. Bloom and Smith (1985), Bienvenue et al. (1982), and Oldfield (1988)]. The lack of change in chain order is also consistent with the results from X-ray diffraction

Table 2: Summary of the Orientations and Dimensions of Lipid and β-Strand Peptide Conformations for Dry Films of DPPC, DMPC, *K27*/DPPC, and *K27*/DMPC, and of DMPC and DPPC Alone, As Determined from ATR-FTIR at 20 °C

		phase			
		DPPC	DMPC	*K27*/DPPC ($R_P = 0.05$)	*K27*/DMPC ($R_P = 0.04$)
lipid	chain tilt angle[a]	32 ± 5	31 ± 7	31 ± 4	32 ± 5
	D_{CH} (Å)[b]	35 ± 2	31 ± 3	36 ± 2	31 ± 2
	D_L (Å)[c]	49 ± 4	46 ± 5	50 ± 4	45 ± 4
β-strand	strand tilt angle[d] (deg)	N/A	N/A	56 ± 3	56 ± 3
	L_P (Å)[e]	N/A	N/A	49 ± 4	49 ± 4
	a_P (Å)[f]	N/A	N/A	79 ± 11	79 ± 11

[a] All tilt angles for the lipid chains in the gel phase are based on the assumption that the angle between the absorption dipole moment of the CH_2 stretching band and the long axis of the hydrocarbon chains is 90° (Fringeli & Günthard, 1981). [b] For determination of the hydrocarbon layer thickness of the bilayer, D_{CH}, in the gel phase, the rise per CH_2 group in ordered hydrocarbon chains is taken to be 1.27 Å. Hence $D_{CH} = 2[1.27(n - 1)\cos\vartheta + L_{C-H}] + L_{H\cdots H}$, where n is the number of carbon atoms in each lipid chain (including position 1), L_{C-H} is the length of a C−H single bond, to take account of the terminal methyl group (taken to be 1.09 Å), $L_{H\cdots H}$ is the H−H van der Waals radius, to take account of the separation of the terminal methyl groups in each monolayer (taken to be 1.0 Å), and ϑ is the tilt angle of the chains. [c] In estimating the bilayer thickness, D_L, the length of the headgroup region in PC bilayers (ordered and disordered) to the center of the glycerol backbone, is taken to be 7 ± 1 Å. Hence, $D_L = D_{CH} + 14$ Å. [d] All tilt angles for the β-strand peptide are calculated taking the angle between the resultant amide II transition moment and the peptide strand axis to be 0°. [e] L_P, the length, projected onto the bilayer normal, of the β-strand (neglecting the contributions from the amide and carbonyl groups at the termini), is taken to be 87 Å (26 × 3.35 Å rise per residue). [f] In estimating a_P, the area per β-strand projected onto the bilayer surface, the specific volume of the peptide is taken to be 0.75 ± 0.05 mL/g; hence, the volume of the peptide (again neglecting the contributions from the amide and carbonyl groups at the termini), ν_P, is taken to be 3856 Å^3 ($[M_R - M_{COOH} - M_{NH2}] \times 0.75/N_A$, where the molar mass, M_R, is 3156 g and M_{COOH} and M_{NH2}, the molar masses of the carbonyl and amide groups, are taken to be 45 g and 16 g, respectively).

that indicate little change of the lipid surface area in the peptide complexes relative to pure lipid bilayers. The results with the *K27* peptide contrast with the effects that some other peptides, such as gramicidin, have on the lipid chain order (Rice & Oldfield, 1979; Watnick & Chan, 1990). However, it should be noted that the magnitude and sign of the ordering effect in these cases are sensitively dependent on lipid chain length (Watnick & Chan, 1990).

The nonoriented FTIR spectra indicate that the peptide is predominantly in the β-strand conformation in the complexes at the relatively high peptide/lipid ratios studied ($R_P = 0.12$ for ESR; $R_P = 0.2$ for DSC, NMR, and X-ray diffraction). A summary of the ATR-IR-derived values for the orientations of the peptide and lipid chain molecular axes, with respect to the surface normal of the ATR crystal (and of the bilayer), is given in Table 2 for dry films of DMPC/*K27* and DPPC/*K27*, together with the chain orientations for pure DPPC and DMPC dry films. Also included in the table are values of the surface area per peptide monomer and the length of the peptide projected onto the bilayer normal, as well as the estimated hydrocarbon layer thickness (D_{CH}). The strands of the β-sheet are strongly tilted relative to the membrane normal, in order to accommodate the relatively long apolar stretch of the peptide within the lipid bilayer (cf. Table 2). A consequence of this is that approximately four lipids per monomer could be accommodated at the two intramembranous surfaces of the β-sheets, if these are not aggregated or form enclosed barrel-type structures [cf. Marsh (1993)]. The somewhat lower lipid/peptide stoichiometry (approximately 2−3 mol/mol) found for the motionally restricted spin-labeled lipid component, and for the effective number of lipids removed from the chain-melting transition in the calorimetry studies, therefore suggests that the β-sheets are to a certain extent associated or present as some form of enclosed structure. The effective projected surface area per peptide monomer, a_P, deduced from the X-ray diffraction measurements, has a value of 112 ± 22 Å^2. This is somewhat different from that estimated for the projected area of the peptide strand itself in dry films of both DMPC and DPPC (79 ± 14 Å^2, see Table 2), which could be consistent with the presence of an aqueous pore associated with the *K27* β-sheet structure. However, it should be pointed out that this difference lies practically within the combined error ranges. If no aqueous pore is associated with the *K27* β-sheet structure, then the decreased lipid stoichiometry found experimentally probably would arise from a limited degree of aggregation of the β-sheet structures, such that closer to one (possibly shared) layer, rather than two independent layers, of lipid is directly associated with the intramembranous surface of the peptide.

The dimensional data shown in Table 2 allow conclusions to be drawn on the way in which the *K27* peptide is incorporated vertically into the bilayer. In the case of the dry film of DPPC, it can be seen that the projected length of a β-strand is comparable with that of the bilayer thickness, while in the DMPC dry film there appears to be a slight mismatch. The observation that the presence of the peptide has no significant effect upon the chain tilt angle of either lipid suggests that the coupling between lipid and peptide is weak in the dry film phase (this may be due to a greater degree of peptide aggregation below the lipid phase transition). Hence, changes in bilayer thickness in the dry film have little influence upon the tilt angle of the β-strands. In the fluid phase (of DMPC) where, presumably, there is not the peptide aggregation/phase separation postulated for the dry film and gel phase, some limited change in peptide orientation may be possible.

CONCLUSION

When incorporated into DMPC and DPPC membranes by dialysis from organic solvents, *K27* has been shown by FTIR spectroscopy to adopt a predominantly β-strand conformation. The incorporation of the peptide has been revealed by ^{2}H NMR spectroscopy to have little effect on the order of the DMPC hydrocarbon chains above the phase transition but does slow their rate of motion. A similar slowing of the lipid headgroup motion was suggested from ^{31}P NMR spectroscopy, which also indicated that the presence of the peptide has a slight disordering effect on the polar region of the lipid. Further evidence for interaction between the lipid and peptide comes from ESR spectroscopy which indicates that on average each peptide molecule motionally restricts between two and three lipid molecules. A similar conclusion was draw from calorimetric observations which also revealed that the peptide causes the abolition of the gel ↔ ripple phase transition and a significant reduction in the cooperativity of the chain melting transition in DMPC.

Utilizing low-angle X-ray diffraction and ^{2}H NMR spectroscopy, the average area of a peptide molecule at the surface of the fluid DMPC bilayer was determined to be 112 $\pm$ 22 Å^2. The magnitude of this value is consistent with the results from ATR-FTIR spectroscopy which showed that in dry peptide/lipid films the β-strands of *K27* are strongly tilted ($\sim$56°), and that, for DMPC at least, the value of this tilt angle is unchanged by hydration in the gel phase but does change upon melting of the lipid chains, presumably because of the flexibility of the bilayer produced by chain fluidization.

ACKNOWLEDGMENT

We thank Dr. T. K. Attwood and Mr. M. Kelly for many helpful discussions. The help of Drs. I. Hooper, J. N. Keen, and J. L. Johnson with peptide synthesis, purification, and analysis and Dr. T. Heimberg with FTIR is acknowledged.

REFERENCES

Ahn, D. J., & Frances, E. I. (1992) *J. Phys. Chem. 96*, 9952−9959.
Barrow, C. J., & Zagorski, M. G. (1991) *Science 253*, 179−182.
Bartlett, G. R. (1959) *J. Biol. Chem. 234*, 466−468.
Bienvenue, A., Bloom, M., Davis, J. H., & Devaux, P. F. (1982) *J. Biol. Chem. 257*, 3032−3038.
Bloom, M., & Smith, I. C. P. (1985) in *Progress in Protein−Lipid Interactions* (Watts, A., & De Pont, J. J. H. H. M., Eds.) Vol. 1, pp 61−88, Elsevier, Amsterdam.
Boden, N., Jones, S. A., & Sixl, F. (1991) *Biochemistry 30*, 2146−2155.
Bogusz, S., Boxer, A., & Busath, D. D. (1992) *Protein Eng. 5*, 285−293.
Branden, C., & Tooze, J. (1991) in *Introduction to Protein Structure*, Garland Publishing Inc., New York & London.
Brophy, P. J., Horváth, L. I., & Marsh, D. (1984) *Biochemistry 23*, 860−865.
Byler, D. M., & Susi, H. (1986) *Biopolymers 25*, 469−487.
Chapman, D. (1983) in *Membrane Fluidity in Biology* (Aloia, R. C., Ed.) Vol. 2, pp 5−42, Academic Press, New York.
Chapman, D., Cornell, B. A., Eliasz, A. W., & Perry, A. (1977) *J. Mol. Biol. 113*, 517−538.
Cross, T. A., & Opella, C. J. (1994) *Curr. Opin. Struct. Biol. 4*, 574−581.
Davis, J. H. (1983) *Biochim. Biophys. Acta 737*, 117−171.
Eibl, H., & Lands, W. E. M. (1969) *Anal. Biochem. 30*, 51−57.
Fischbarg, J., Cheung, M., Czeglady, F., Li, J., Iserovich, P., Kuang, K., Hubbard, J., Garner, M., Rosen, D. M., Golde, D. W., & Vena, J. C. (1993) *Proc. Natl. Acad. Sci. U.S.A. 90*, 11658−11662.
Fraser, R. D. B., & MacRae, T. P. (1973) in *Conformations in Fibrous Proteins and Related Synthetic Polypeptides*, p 628, Academic Press, New York.
Frey, S., & Tamm, L. K. (1991) *Biophys. J. 60*, 922−930.
Fringeli, U. P. (1977) *Z. Naturforsch., C: Biosci. 32C*, 20−45.
Fringeli, U. P., & Günthard, H. H. (1981) in *Membrane Spectroscopy* (Grelll, E., Ed.) pp 290−332, Springer-Verlag, Berlin, Heidelberg, and New York.
Gremlich, H. U., Fringeli, U. P., & Schwyzer, R. (1983) *Biochemistry 22*, 4257−4264.
Gupta, C. M., Radhakrishnan, R., & Khorana, H. G. (1977) *Proc. Natl. Acad. Sci. U.S.A. 74*, 4315−4319.
Guttman, C. M., & Flynn, J. H. (1973) *Anal. Chem. 45*, 408−410.
Hirs, C. H. W. (1967) *Methods Enzymol. 11*, 325−329.
Janiak, M. J., Small, D. M., & Shipley, G. G. (1976) *Biochemistry 15*, 4575−4580.
Janiak, M. J., Small, D. M., & Shipley, G. G. (1979) *J. Biol. Chem. 13*, 6068−6078.
King, D. S., Fields, C. G., & Fields, G. B. (1990) *Int. J. Pept. Protein Res. 36*, 255−266.
Krimm, S., & Bandekar, J. (1986) *Adv. Protein Chem. 38*, 181−364.
Lowry, O. H., Rosenbrough, N. J., Farr, A. C., & Randall, R. J. (1951) *J. Biol. Chem. 193*, 265−275.
Luzzati, V. (1968) in *Biological Membranes* (Chapman, D., Ed.) Vol. 1, pp 71−123, Academic Press, New York.
Marsh, D. (1981) in *Membrane Spectroscopy* (Grell, E., Ed.) pp 51−142, Springer-Verlag, Berlin, Heidelberg, and New York.
Marsh, D. (1982) *Tech. Life Sci.: Biochem. B4/II*, B426/1−B426/44.
Marsh, D. (1985) in *Progress in Protein−Lipid Interactions* (Watts, A., & De Pont, J. J. H. H. M., Eds.) Vol. 1, pp 143−172, Elsevier, Amsterdam.
Marsh, D. (1993) in *New Comprehensive Biochemistry: Protein−Lipid Interactions* (Watts, A., Ed.) Vol. 25, pp 41−66, Elsevier, Amsterdam.
Marsh, D., & Watts, A. (1982) in *Lipid−Protein Interactions* (Jost, P. C., & Griffith, O. H., Eds.) Vol. 2, pp 53−126, Wiley-Interscience, New York.
Mason, J. T., Broccoli, A. V., & Huang, C.-H. (1981) *J. Biochem. 113*, 96−101.
Miyazawa, T. (1960) *J. Am. Chem. Soc. 32*, 1647−1652.
Miyazawa, T. (1967) in *Poly-α-Amino Acids. Protein Models for Conformational Studies* (Fasman, G. D., Ed.) pp 69−103, Marcel Dekker, New York.
Miyazawa, T., & Blout, E. R. (1961) *J. Am. Chem. Soc. 83*, 712−719.
Nagle, J. F., & Wilkinson, D. A. (1978) *Biophys. J. 23*, 159−175.
Ohta, K., & Iwamoto, R. (1985) *Appl. Spectrosc. 39*, 418−425.
Oldfield, E. (1988) *Biochem. Soc. Trans. 16*, 1−10.
Pan, K. M., Baldwin, M., Nguyen, J., Gasset, M., Serban, A., Groth, D., Mehlhorn, I., Huang, Z., Fletterick, R. J., Cohen, F. Z., & Prusiner, S. B. (1993) *Proc. Natl. Acad. Sci. U.S.A. 90*, 10962−10966.
Peelen, S. J. C. J., Sanders, J. C., Hemminga, M. A., & Marsh, D. (1992) *Biochemistry 31*, 2670−2677.
Prusiner, S. B. (1991) *Science 252*, 1515−1522.
Rice, D., & Oldfield, E. (1979) *Biochemistry 18*, 3272−3279.
Sandbank, B. M. (1986) Ph.D. Thesis, Department of Biophysics, University of Leeds.
Seelig, J. (1978) *Biochim. Biophys. Acta 515*, 105−140.
Seelig, J., & Seelig, A. (1980) *Q. Rev. Biophys. 13*, 19−61.
Smith, P. K., Krohn, R. I., Henmanson, G. T., Mallia, A. K., Gartner, F. H., Provenzano, M. D., Fujimoto, E. K., Goeke, N. M., Olson, B. J., & Klenk, D. C. (1985) *Anal. Biochem. 150*, 76−85.
Surewicz, W. K., & Mantsch, H. H. (1988) *Biochim. Biophys. 952*, 115−130.
Surewicz, W. K., Mantsch, H. H., & Chapman, D. (1993) *Biochemistry 32*, 389−394.
Takumi, T., Ohkubo, H., & Nakanishi, S. (1988) *Science 242*, 1042−1045.
Unwin, N. (1993) *J. Mol. Biol. 229*, 1101−1124.
Watnick, P. I., & Chan, S. I. (1990) *Biochemistry 29*, 6215−6221.
Weiss, M. S., Kreusch, A., Schiltz, E., Nestel, U., Welte, W., Weckesser, J., & Schulz, G. E. (1991) *FEBS Lett. 280*, 379−382.
Yellen, G., Jurman, M., Abramson, T., & Mackinnon, R. (1991) *Science 251*, 939−942.
Zbinden, R. (1964) in *Infrared Spectroscopy of High Polymers*, Academic Press, New York.

BI960891G